Electronic Supplementary Material (ESI) for Dalton Transactions

Supporting information

Homoleptic 1-D Iron Selenolate Complexes — Synthesis, Structure, Magnetic and Thermal Behaviour of $^{1}_{\infty}$[Fe(SeR)$_2$] (R = Ph, Mes)**

Andreas Eichhöfer[a]*, Gernot Buth[b], Francesco Dolci[c], Karin Fink[a], Richard. A. Mole[d], Paul T. Wood[e]

[a] Institut für Nanotechnologie and [b] Institut für Synchrotronstrahlung; Karlsruhe Institut für Technologie (KIT)Postfach 364076021 Karlsruhe (Germany)

[c] European Commission - JRC Institute for Energy Cleaner Energy Unit, Westerduinweg 3, NL-1755 ZG Petten, The Netherlands

[d] ZWE FRM-II, Lichtenbergstrasse 1, 85747 Garching, Germany

[e] University Chemical Laboratory, Lensfield Rd., Cambridge CB2 1EW (UK)

**(Ph = phenyl = C_6H_5, Mes = mesityl = C_6H_2-2,4,6-$(CH_3)_3$)

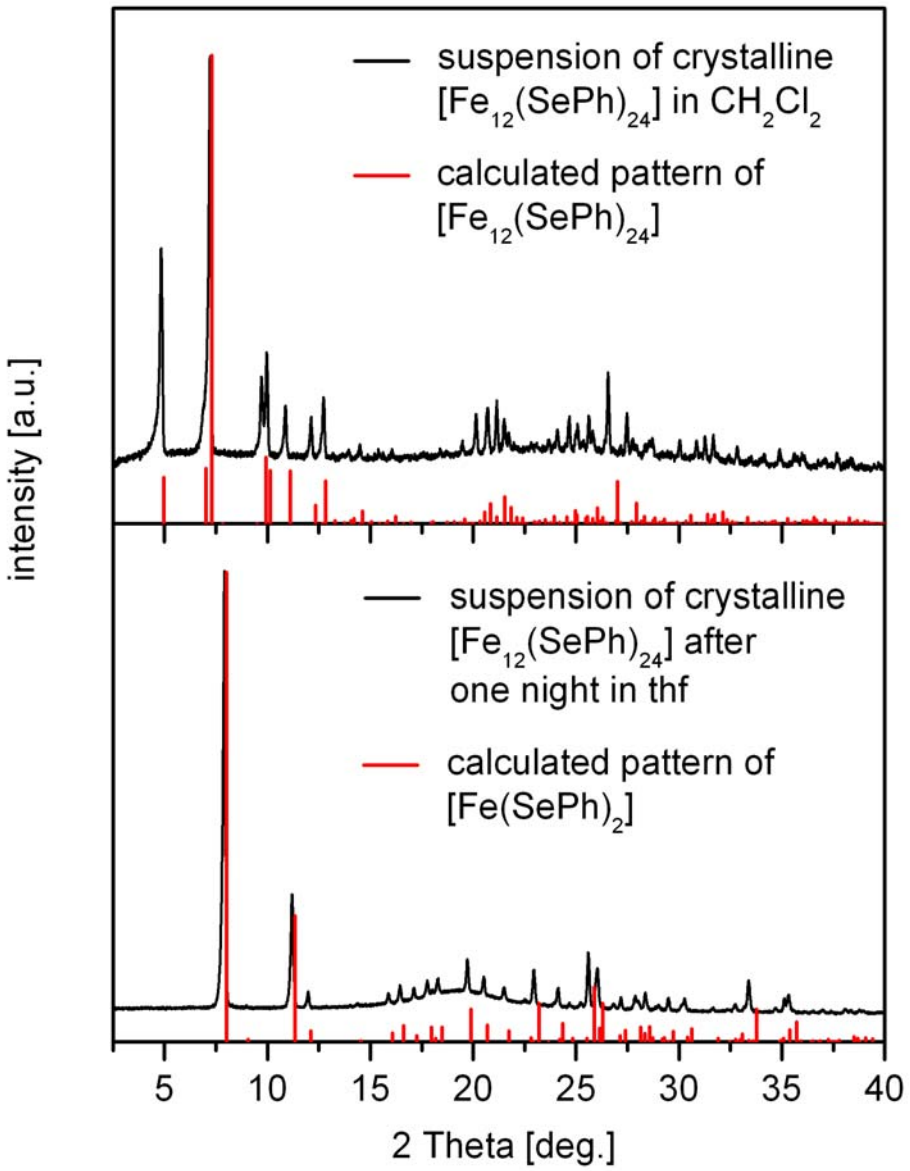

Figure S1. Measured (black) and simulated (red) X-ray powder patterns of $[Fe(SePh)_2]_{12}$ as a suspension of fresh crystals in CH_2Cl_2 (up) and as a suspension of crystals after one night in thf compared with the calculated pattern of $^{1}_{\infty}[Fe(SePh)_2]$ (**1**) (down).

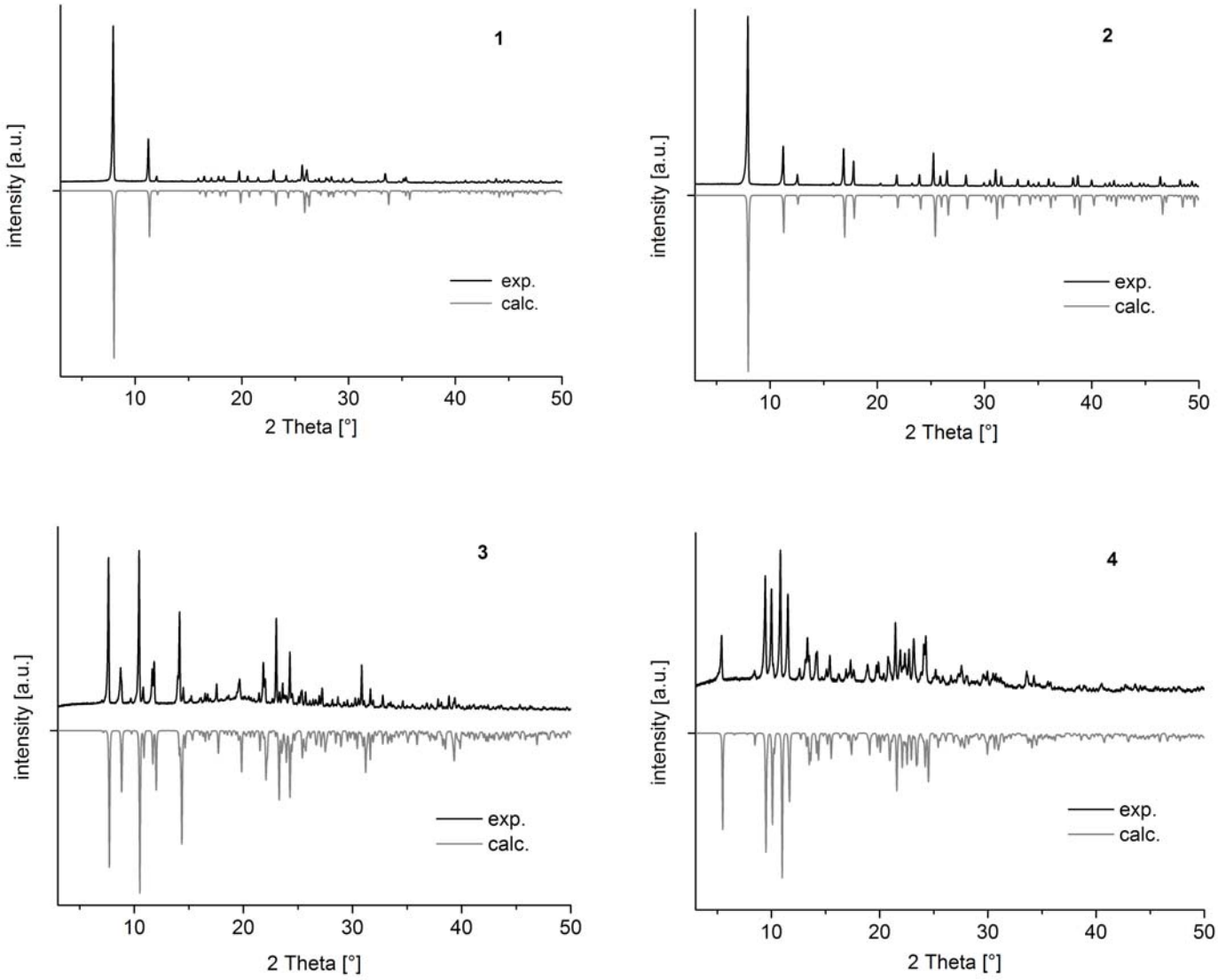

Figure S2. Measured (black) and simulated (grey) X-ray powder patterns of $^{1}_{\infty}[Fe(SePh)_2]$ (**1**), $^{1}_{\infty}[Fe(SeC_6H_2(CH_3)_3)_2]$ (**2**), $[Fe(SePh)_2(1,10\text{–}phen)_2]$ (**3**) and $[Fe(phen)_3][Fe(SePh)_4]$ (**4**).

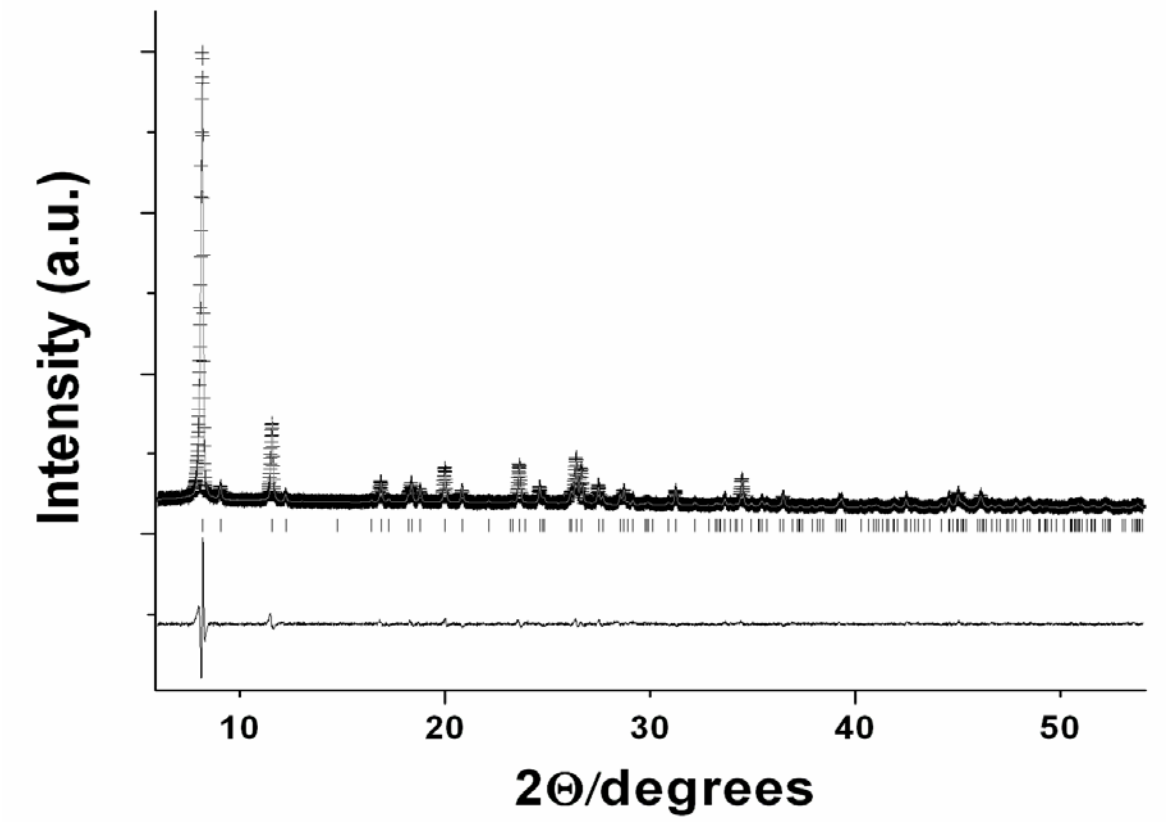

Figure S3. Rietveld refinement results for **1** after thermal treatment. Observed (cross symbols), calculated and difference profiles are present in figure. Weighted R value-Rw% is 4.48. Goodness of fit-chi^2 is 2.04.

Table S1. Refined parameters for **1** after heat treatment. The space group number is $I4_1/a$ (No. 88; setting 2). Cell parameters are $a = b = 21.5799(4)$ Å and $c = 10.9024(5)$ Å; $V = 5077.0$ Å^3.

.

Atom Label	Atom Type	X coordinate	Y coordinate	Z coordinate	Biso	Occupancy
Se1	Se	0.7656(5)	0.4118(3)	0.093(1)	4.3(4)	1
Se2	Se	0.674(4)	0.5552(5)	-0.034(1)	2.5(3)	1
Fe1	Fe	0.7714(7)	0.5221(7)	0.029(1)	2.9(3)	1
C1	C	0.8419	0.3846	0.0881	3.81	1
C2	C	0.8501	0.3571	-0.0248	4.81	1
H2	H	0.8169	0.3522	-0.0793	5.8	1
C3	C	0.907	0.3367	-0.0574	6.4	1
H3	H	0.9126	0.3171	-0.1342	7.7	1
C4	C	0.9551	0.3445	0.0193	6.8	1
H4	H	0.994	0.3303	-0.004	8.1	1
C5	C	0.9472	0.3728	0.1302	7	1
H5	H	0.981	0.3789	0.1826	8.4	1
C6	C	0.8904	0.3927	0.1667	5.6	1
H6	H	0.8849	0.4114	0.2444	6.7	1
C7	C	0.6882	0.642	0.0183	4.3	1
C8	C	0.7031	0.6817	-0.0763	5.18	1
H8	H	0.7085	0.6667	-0.1574	6.2	1
C9	C	0.71	0.7427	-0.0528	5.9	1
H9	H	0.7207	0.7696	-0.1173	7	1
C10	C	0.7014	0.7648	0.0658	6.3	1
H10	H	0.7053	0.8068	0.0823	7.5	1
C11	C	0.6872	0.7253	0.1588	6.6	1
H11	H	0.6821	0.7402	0.24	7.9	1
C12	C	0.6801	0.6639	0.1356	5.59	1
H12	H	0.6698	0.6371	0.2005	6.7	1

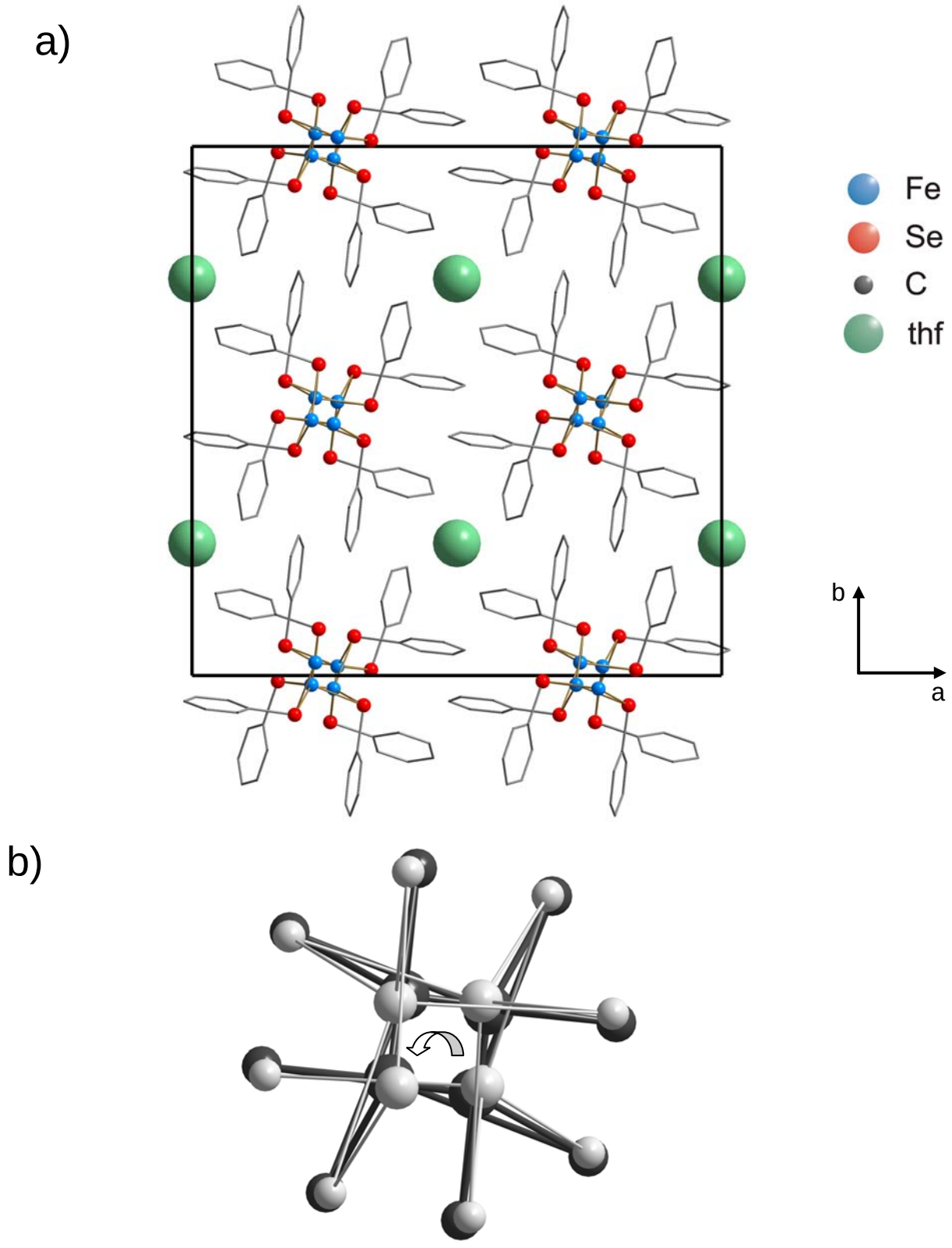

Figure S4. a) Structure of $^{1}_{\infty}$[Fe(SePh)$_2$] (**1**) in the crystal, view along *c*, location of the channels of disordered thf molecules are schematically indicated by the green balls; b) irreversible twist of the FeSe-chains in **1** before (black) and after (light grey) heating to 110 °C and cooling down.

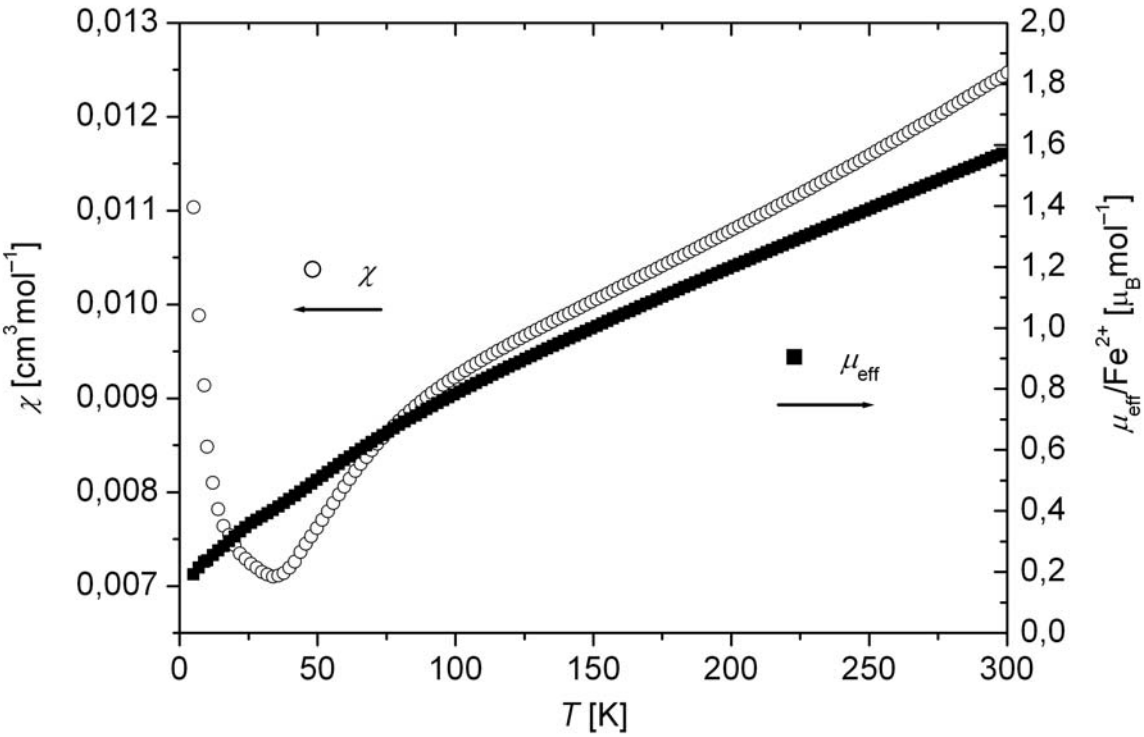

Figure S5. Susceptibility behaviour for $[Fe(SePh)_2]_{12}$.

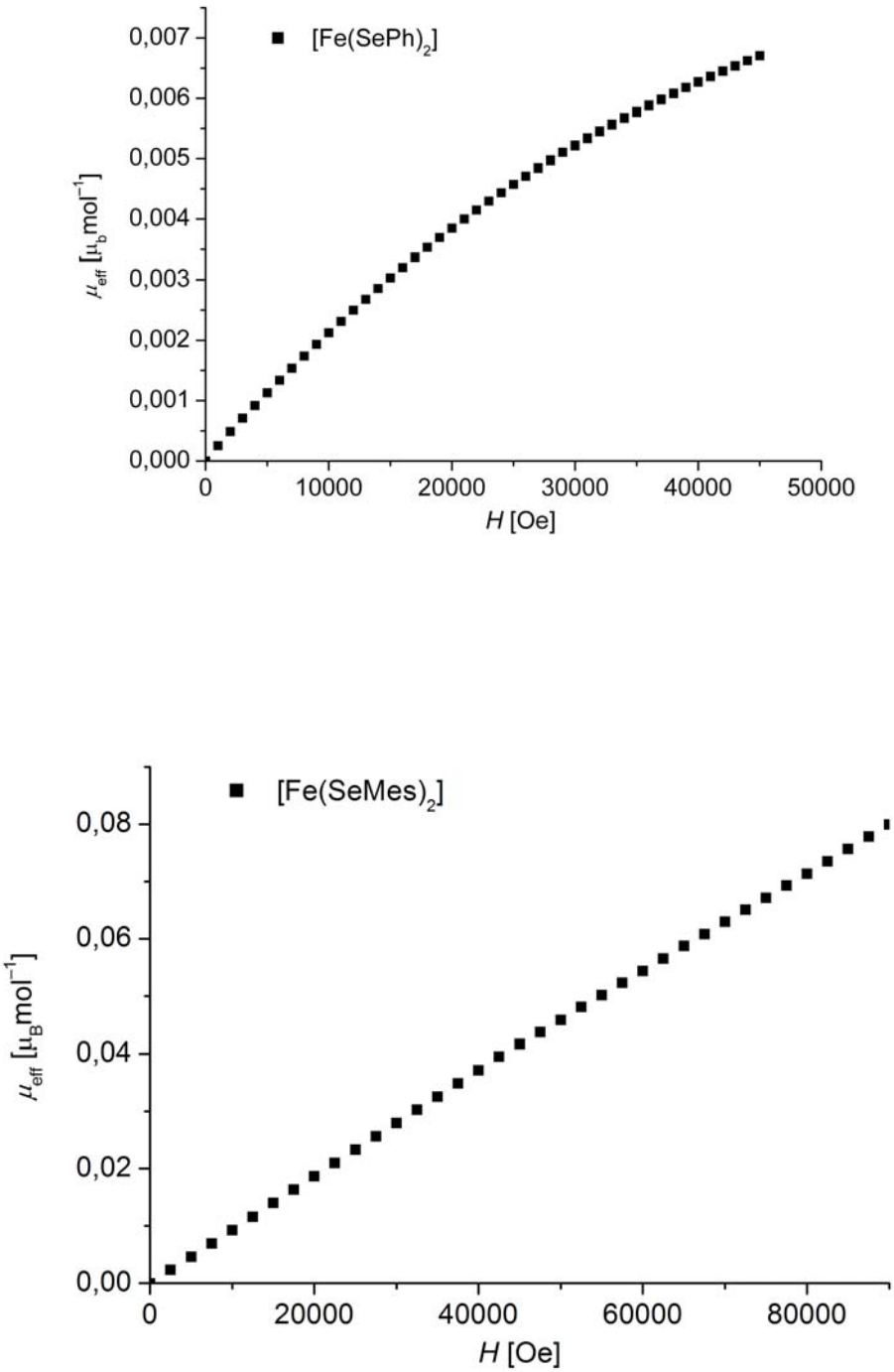

Figure S6. Isothermal magnetization curves of $^{1}_{\infty}[Fe(SePh)_2]$ (**1**) and $^{1}_{\infty}[Fe(SeC_6H_2(CH_3)_3)_2]$ (**2**) at 5K.

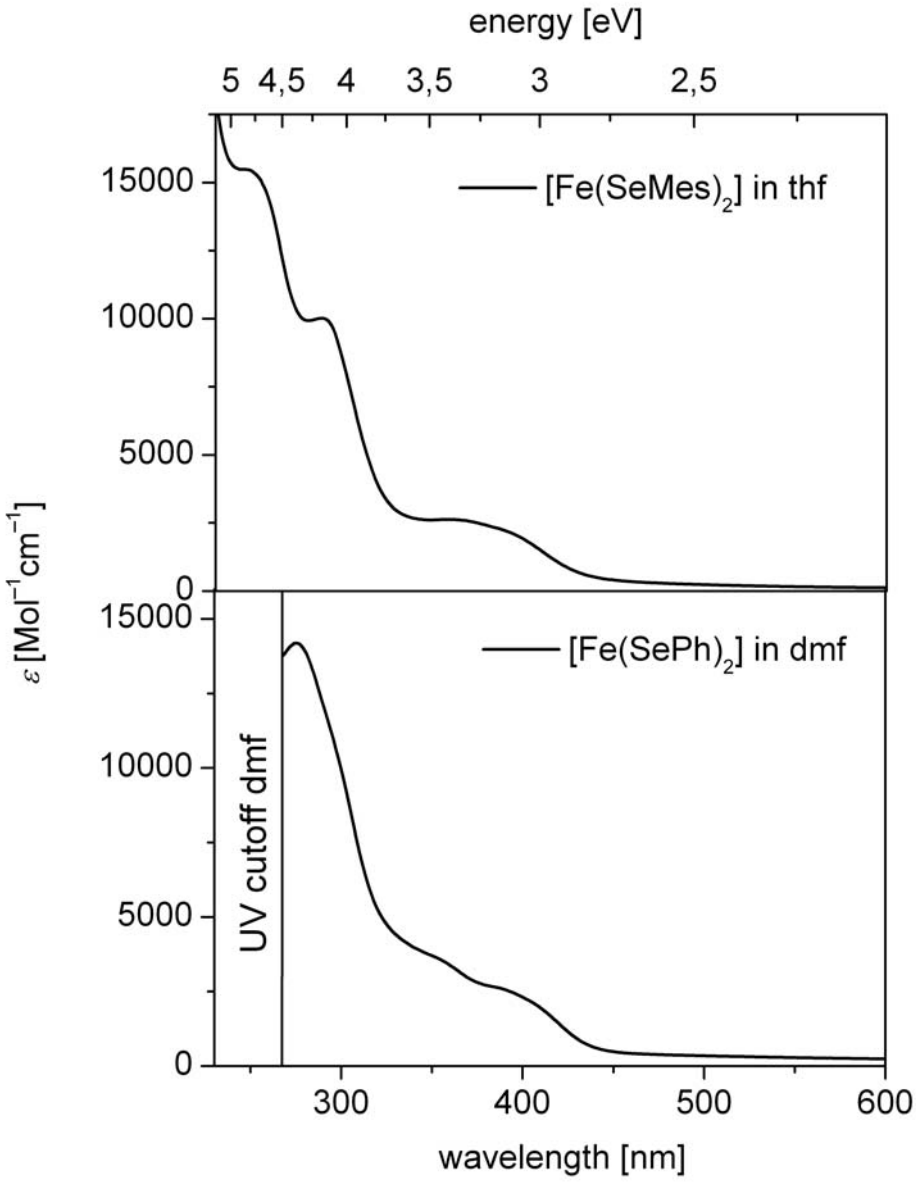

Figure S7. UV-Vis spectra of $^{1}_{\infty}[Fe(SePh)_2]$ (**1**) and $^{1}_{\infty}[Fe(SeC_6H_2(CH_3)_3)_2]$ (**2**) in solution.

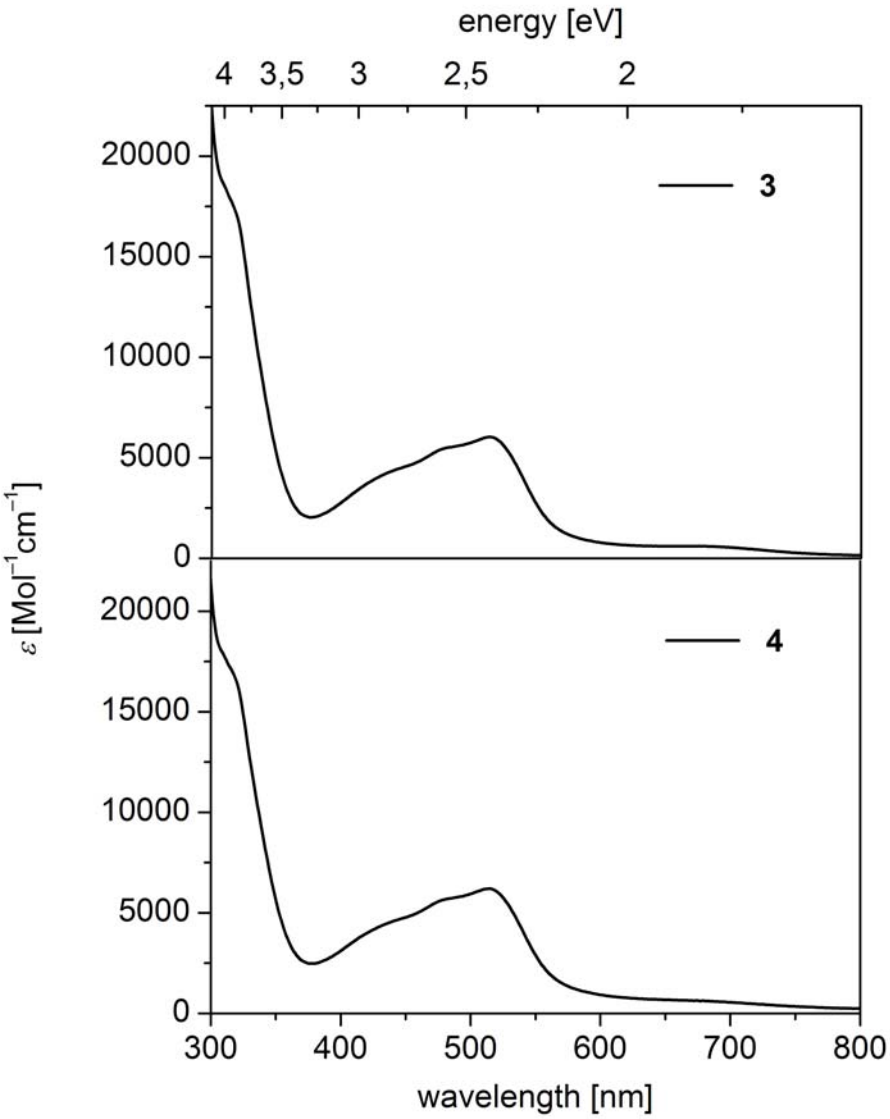

Figure S8. UV-Vis spectra of $[Fe(SePh)_2(1,10–phen)_2]$ (**3**) and $[Fe(phen)_3][Fe(SePh)_4]$ (**4**) in dmf.

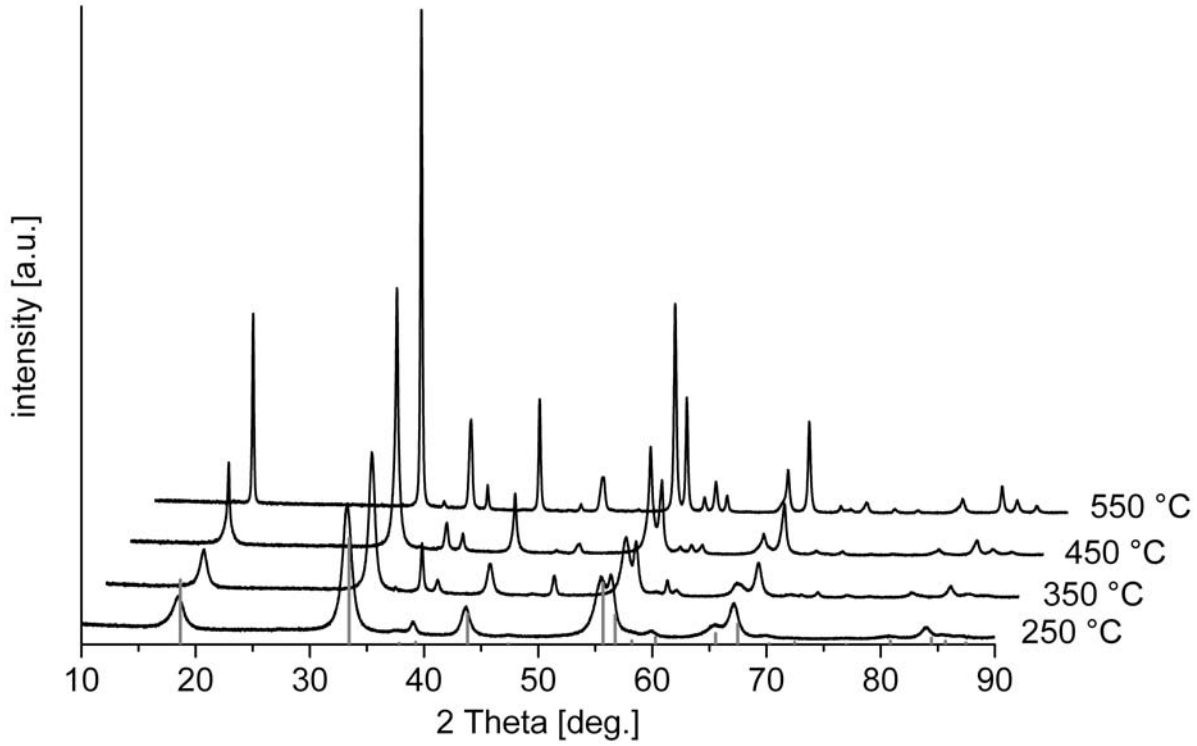

Figure S9. Powder XRD patterns of the residue of $^{1}_{\infty}$[Fe(SePh)$_2$] (**1**) after thermal treatment at 250, 350, 450 and 550 °C under vacuum ($3 \cdot 10^{-6}$ mbar) compared to the indexed reflection patterns of tetragonal $Fe_{1+x}Se$ ($0.012 < x < 0.02$) [13] (grey lines).